INSTITUTE OF PHYSICS PUBLISHING NANOTECHNOLOGY
Nanotechnology **13** (2002) 120–131 PII: S0957-4484(02)30453-7

Calculation of pull-in voltages for carbon-nanotube-based nanoelectromechanical switches

Marc Dequesnes, S V Rotkin and N R Aluru[1,2]

Beckman Institute for Advanced Science and Technology, University of Illinois at Urbana-Champaign, Urbana, IL 61801, USA

E-mail: aluru@uiuc.edu

Received 2 November 2001
Published 22 January 2002
Online at stacks.iop.org/Nano/13/120

Abstract
We study the pull-in voltage characteristics of several nanotube electromechanical switches, such as double-wall carbon nanotubes suspended over a graphitic ground electrode. We propose parametrized continuum models for three coupled energy domains: the elastostatic energy domain, the electrostatic energy domain and the van der Waals energy domain. We compare the accuracy of the continuum models with atomistic simulations. Numerical simulations based on continuum models closely match the experimental data reported for carbon-nanotube-based nanotweezers. An analytical expression, based on a lumped model, is derived to compute the pull-in voltage of cantilever and fixed–fixed switches. We investigate the significance of van der Waals interactions in the design of nanoelectromechanical switches.

(Some figures in this article are in colour only in the electronic version)

1. Introduction

Nanoelectromechanical systems (NEMS) are sensors, actuators, devices and systems with critical dimensions of the order of nanometres. NEMS are about a thousand times smaller than microelectromechanical systems (MEMS). MEMS technology has already had a significant impact on medical, automobile, aerospace and information technology areas [1]. NEMS have the potential to enable revolutionary technology for these areas. Some prospective applications of NEMS include random access memory [2], nanotweezers for miniaturized robotics and other applications [3] and super-sensitive sensors [4, 5]. NEMS can be designed using a host of materials including silicon, silicon carbide, carbon and other materials.

Carbon nanotubes are promising for the design and development of NEMS not only because of their excellent electronic and mechanical properties, but also because of the significant progress that has been made in the last few years in fabrication of carbon nanostructures. Recent studies have demonstrated the use of carbon nanotubes as memory devices [2], nanomanipulators or nanotweezers [3,6], sensors [4, 5] and actuators [7]. In this paper, we focus on a particular application of carbon nanotubes—namely, nanoelectromechanical (NEM) switches. NEM switches are fundamental building blocks for the design of random access memory, and devices for high-frequency operation and fast switching in communication networks. Because of the difficulties in manufacturing nanostructures, experiments on nanoswitches have been costly. Computational design tools, when sufficiently precise and accurate, can be far more economical than trial-and-error design cycles based purely on experimentation. In this paper, we propose theoretical models for analysis and design of NEM switches.

The operation and design of NEM switches closely resembles the design and operation of microelectromechanical (MEM) switches. Hence, the obvious question is can MEMS theories be used to design NEMS? Because NEM switches are about three orders of magnitude smaller than MEM switches, new physics is encountered when designing NEM switches. Specifically, van der Waals interactions, which can be neglected when designing MEM switches, play an important role in nanoscales. Hence, the use of MEMS models is limited

[1] Corresponding author.
[2] http://www.uiuc.edu/~aluru

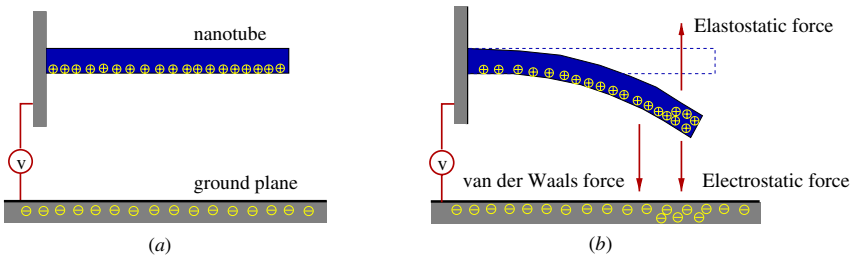

Figure 1. Force balance for a nanotube over a ground plane: (*a*) position of the tube when $V = 0$, (*b*) deformed position of the tube when $V \neq 0$.

and new models need to be developed for analysis and design of NEM switches.

A common approach to nanoscale simulation is to use molecular dynamics (MD). For example, MD or atomistic simulations [8] have been used to probe the mechanical behaviour of nanogears [9]. However, MD simulations require the computation of all atoms of the system. The timestep in MD simulations is typically of the order of 0.1 fs for a stable integration scheme. MD simulations involving more than a million atoms are very expensive and the dynamics of the system can only be probed for a few picoseconds. Therefore, MD simulations may not be easily used in an integrated design process or for design optimization. An alternative approach that is significantly faster than MD is required.

In this paper we raise the question of applicability of continuum theories for nanoscale devices. NEM switches are typically designed with small gaps between the tubes and the ground plane. In such cases, we show that parametrized continuum models can be used reliably to design nanoscale devices. Specifically, we show that the mechanical behaviour of NEM switches can be modelled by parametrized beam models. Similarly, we show that a continuum model can be used to calculate the van der Waals energy, *in lieu* of the discrete Lennard-Jones potential. The contributions of this paper include the following:

- The development of simple continuum models, that are fast and reasonably accurate, for modelling and simulation of NEM switches.
- The development of a continuum model for simulation of the van der Waals interactions.
- The development of an analytical expression, based on a lumped model, to estimate the pull-in voltage of NEM switches.
- The demonstration that the van der Waals interactions play a significant role in determining the pull-in voltage and cannot be neglected in designing NEM switches.

The rest of the paper is organized as follows: the operation of NEM switches is described in section 2. Continuum theoretical models for NEM switches are presented in section 3, the validation of the continuum theories, as well as their limitations, are discussed in section 4, the development of an analytical approach to compute the pull-in voltage is discussed in section 5 and simulation results for several NEM switches are shown in section 6. Finally, conclusions are presented in section 7.

2. Operation of nanoelectromechanical switches

Figure 1 shows the physical operation of a carbon-nanotube-based cantilever switch. The key components are a movable structure, which can be a single-wall or a multiwall carbon nanotube, and a fixed ground plane, which is modelled by a graphite bulk. When a potential difference is created between the movable structure and the ground plane, electrostatic charges are induced on both the movable structure and the ground plane. The electrostatic charges give rise to electrostatic forces, which deflect the movable tube. In addition to electrostatic forces, depending on the gap between the movable tube and the ground plane, van der Waals forces also act on the tube and deflect it. The direction of the electrostatic and van der Waals forces is shown in figure 1. Counteracting the electrostatic and van der Waals forces are elastic forces, which try to restore the tube to its original straight position. For an applied voltage, an equilibrium position of the tube is defined by the balance of the elastic, electrostatic and the van der Waals forces. As the tube deflects, the electrostatic, van der Waals and the elastic forces change, so a self-consistent analysis is necessary to compute the equilibrium position of the tube.

When the applied potential difference between the tube and the ground plane exceeds a certain potential, the tube becomes unstable and collapses onto the ground plane. The potential which causes the tube to collapse onto the ground plane is defined as the pull-in voltage or the collapse voltage. When the pull-in voltage is applied, the tube comes in contact with the ground plane, and the device is said to be in the ON state. When the potential is released and the tube and the ground plane are separated, the device is said to be in the OFF state.

When compared with microelectromechanical switches [10–12], the operation of NEM switches is different because of the importance of the van der Waals forces, which can be neglected at the micrometre scale. The sticking of NEM devices becomes an increasing problem at the nanoscale and can limit the range of operability of NEMS. If the gap between the cantilever tube and the ground plane is very small, even without an applied voltage, the tube can collapse onto the ground plane because of the van der Waals forces. In addition, the separation of the tube from the ground plane after the contact is an issue as the van der Waals forces will tend to keep the tube and the ground plane together. In this paper, we show that the van der Waals forces can have a significant effect on the calculated pull-in voltage of NEM switches.

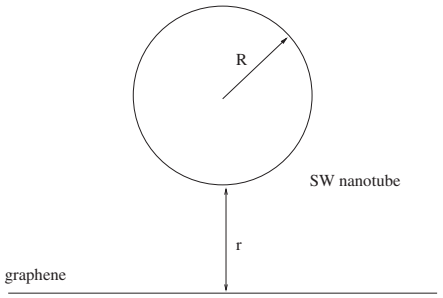

Figure 2. Single-shell continuum geometry: an SWNT over a graphene ground plane.

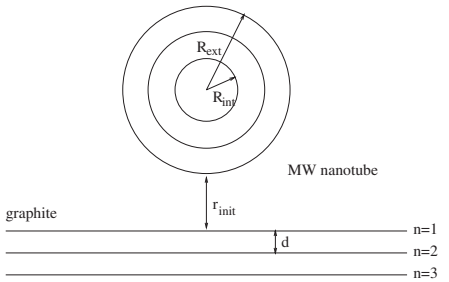

Figure 3. Multiple-shell continuum geometry: an MWNT over a graphite ground plane.

3. Theory

As discussed in section 2, the simulation of NEM switches requires an understanding and analysis of three coupled energy domains: elastostatics, electrostatics and van der Waals interactions. In this section, we discuss continuum models for each of these energy domains. The validity of these models for simulation of NEMS is discussed in section 4.

3.1. van der Waals interactions

The van der Waals energy can be computed by using the well known Lennard-Jones potential [13], which has an attractive term and a repulsive term. The repulsive part of the potential decays extremely fast and plays an important role only after the nanotube has come in contact with the ground plane. The repulsive part is negligible before the collapse and, hence, is dropped in the following discussion. The Lennard-Jones potential describing an attractive interaction between two atoms i and j is given by

$$\phi_{ij} = -\frac{\mathcal{C}_6}{r_{ij}^6} \tag{1}$$

where r_{ij} is the distance between atoms i and j and $\mathcal{C}_6$ is a constant characterizing the interactions between the two atoms. For example, for a carbon–carbon interaction the value of $\mathcal{C}_6$ is 15.2 eV Å^6 [14]. Using equation (1), the total van der Waals energy can be computed by a pairwise summation over all the atoms, which costs about $O(n^2)$ operations, where n is the number of atoms.

An alternative approach to compute the total van der Waals energy is to employ a continuum model [15]. In the continuum model, the total van der Waals energy is computed by the double volume (or surface) integral of the Lennard-Jones potential, i.e.

$$E_{\mathrm{vdW}}(r) = \int_{\mathcal{V}_1}\int_{\mathcal{V}_2} \frac{n_1 n_2 \mathcal{C}_6}{r^6(\mathcal{V}_1, \mathcal{V}_2)}\,\mathrm{d}\mathcal{V}_1\,\mathrm{d}\mathcal{V}_2 \tag{2}$$

where $\mathcal{V}_1$ and $\mathcal{V}_2$ represent the two domains of integration, and n_1 and n_2 are the densities of atoms for the domains $\mathcal{V}_1$ and $\mathcal{V}_2$, respectively. For example, $\mathcal{V}_1$ is the volume of the nanotube and $\mathcal{V}_2$ is the bulk representing the graphite ground plane. $r^6(\mathcal{V}_1, \mathcal{V}_2)$ is the distance between any point on $\mathcal{V}_1$ and any point on $\mathcal{V}_2$.

Consider the interaction of a tube with a ground plane as shown in figure 1. Assuming that the tube is a single-wall nanotube (SWNT) and the ground plane is a single monolayer of graphite (graphene) (see figure 2), the van der Waals energy can be computed by performing an integration over the surfaces of the shell and the graphene. In this case, n_1 and n_2 are the same graphite surface density of atoms and the integration gives an energy per unit length of the nanotube as

$$\frac{E_{\mathrm{vdW}}}{L} = \frac{\mathcal{C}_6\sigma^2\pi^2 R(R+r)(3R^2+2(r+R)^2)}{2((r+R)^2-R^2)^{7/2}} \tag{3}$$

where $\sigma \simeq 38\ \mathrm{nm}^{-2}$ is the graphite surface density, L is the length of the nanotube, R is the radius of the nanotube and r is the distance between the bottom wall of the nanotube and the graphene sheet.

To compute the interaction of a multiwall nanotube (MWNT) with bulk graphite (see figure 3) we sum the terms defining the interaction between all separate shells and layers. For an MWNT, the energy per unit length is given by

$$\frac{E_{\mathrm{vdW}}}{L} = \sum_{R=R_{\mathrm{int}}}^{R_{\mathrm{ext}}} \sum_{r=r_{\mathrm{init}}}^{(n-1)\times d+r_{\mathrm{init}}} \times \frac{\mathcal{C}_6\sigma^2\pi^2 R(R+r)(3R^2+2(r+R)^2)}{2((r+R)^2-R^2)^{7/2}} \tag{4}$$

where R_{int} and R_{ext} are the inner and the outer radius of the nanotube, respectively, n is the number of graphene layers of the substrate, $d = 3.35$ Å is the interlayer distance of graphite and r_{init} is the gap between the outer wall of the nanotube and the surface layer of graphite.

Once the van der Waals energy is computed, the van der Waals force per unit length is computed by

$$q_{\mathrm{vdW}} = \frac{\mathrm{d}\left(\frac{E_{\mathrm{vdW}}}{L}\right)}{\mathrm{d}r} = \sum_{R=R_{\mathrm{int}}}^{R_{\mathrm{ext}}} \sum_{r=r_{\mathrm{init}}}^{(n-1)\times d+r_{\mathrm{init}}} -\left(\mathcal{C}_6\sigma^2\pi^2 R\sqrt{r(r+2R)} \times (8r^4+32r^3R+72r^2R^2+80rR^3+35R^4)\right) \times \{2r^5(r+2R)^5\}^{-1}. \tag{5}$$

3.2. Electrostatic forces

The electrostatic forces are computed by using a standard capacitance model [16]. The nanotube is approximated as a perfect cylindrical conductor. This implies that the potential is constant along the length of the tube. This assumption is valid for MWNTs but may need a correction for SWNTs. The capacitance for a twin-lead system, i.e.

Figure 4. Comparison of the deflection of a 20 nm long fixed–fixed DWNT (diameter of 1.96 nm) with the deflection predicted by the beam equation. The solid black curve is the deflection predicted by the beam equation.

for cylinders that are oppositely charged, is given in [17]. The twin-lead wire problem has the same electric field as a cylinder over a ground plane, because the presence of the ground plane is equivalent to the presence of an imaginary cylinder with an opposite charge mirrored in the plane. Then, the capacitance per unit length for the cylindrical beam over the conductive ground plane is given by

$$C(r) = \frac{\pi\epsilon_0}{\log\left[1 + \frac{r}{R} + \sqrt{\left(\frac{r}{R}+1\right)^2 - 1}\right]} \tag{6}$$

where R is the radius of the cylinder/conductor ($R = R_{\text{ext}}$ for MWNT), r is the gap between the conductor and the ground plane ($r = r_{\text{init}}$ for the configuration shown in figure 3) and ϵ_0 is the permittivity of vacuum.

The electrostatic energy per unit length is given by $E_{\text{elec}}/L = CV^2/2$. The electrostatic force per unit length, q_{elec}, is then given by

$$q_{\text{elec}} = \frac{\mathrm{d}\left(\frac{E_{\text{elec}}}{L}\right)}{\mathrm{d}r} = -\frac{\pi\epsilon_0 V^2}{R\sqrt{\frac{r(r+2R)}{R^2}}\log^2\left[1 + \frac{r}{R} + \sqrt{\frac{r(r+2R)}{R^2}}\right]}. \tag{7}$$

3.3. Elastostatic domain

The mechanical behaviour of the nanotube is approximated by a continuum beam equation, i.e.

$$EI\frac{\mathrm{d}^4 r}{\mathrm{d}x^4} = q \tag{8}$$

where r is the gap between the conductor and the ground plane, x is the position along the tube, q is the force per unit length acting normal to the beam, E is the Young's modulus, I is the moment of inertia and for nanotubes I can be estimated as

$$I = \pi/4 \times (R_{\text{ext}}^4 - R_{\text{int}}^4) \tag{9}$$

where R_{int} is the interior radius and R_{ext} is the exterior radius.

3.4. Governing equation for NEM switches

The pull-in voltage of the nanocantilever and the fixed–fixed tube device can be determined by coupling the electrostatic, van der Waals and elastostatic domains into a single equation, i.e.

$$EI\frac{\mathrm{d}^4 r}{\mathrm{d}x^4} = q_{\text{elec}} + q_{\text{vdW}}. \tag{10}$$

The expressions for q_{vdW} and q_{elec} are given in equations (5) and (7), respectively. The governing equation is nonlinear, which means that it is not possible, in general, to come up with an analytical solution. It is to be solved self-consistently to compute the equilibrium position of the nanotubes. Starting with an initial guess for the deflection of the tube, the forces are computed and, then, are used to solve the equation to compute a new deflection of the tube. These steps are repeated until a converged solution is obtained.

4. Validity and limitations of the continuum theory

The validity of the continuum theory presented in the previous section needs to be addressed before it can be applied to model NEM switches. In this section we compare the beam theory for nanotubes with MD simulations and the continuum theory for the van der Waals interactions with the discrete Lennard-Jones potential.

4.1. Comparison of beam theory with molecular dynamics simulations

The continuum beam theory has been used widely to model the mechanics of nanotubes [18, 19]. MD simulations can be very useful to establish the accuracy of continuum theories. In this section, we test the accuracy of beam theories for MWNTs with MD simulations.

MD simulations have been performed on a double-wall nanotube (DWNT) with a diameter of 1.96 nm and a length of 20 nm at 10 K. The DWNT considered is made of a (25, 0) tube for the outer shell and a (16, 0) tube for the inner shell. The time integration was performed with a velocity Verlet algorithm [20]. The simulation time was in the range of 100 ps with a timestep of 0.1 fs. The bonded interactions are modelled with a Brenner potential with a parametrization for graphite [21]. The non-bonded interactions are considered between the tube walls only and are modelled by the Lennard-Jones potential [14]. The non-bonded interactions prevent the nanotube walls from overlapping. For a uniformly distributed load of 1.8 N m^{-1}, the comparison between the beam theory given in equation (8) and the MD simulations is shown in figure 4. The agreement is excellent for an I computed by using equation (9), where $R_{\text{int}} = 6.3$ Å and $R_{\text{ext}} = 9.8$ Å. The Young's modulus was set to be 1.2 TPa as determined from the MD simulations.

To determine the Young's modulus, the peak deflection of the tube as a function of the applied load is plotted as shown in figure 5. A continuum model approximation for the load–deflection curve shown in figure 5 requires the slope to be equal to $L^4/(384EI)$, where L is the length of the tube. From the slope of the MD load–deflection curve, the Young's modulus of the tube is retrieved to be $E \simeq 1.2$ TPa. This value is consistent with the theoretical and experimental data published previously [19, 22–26].

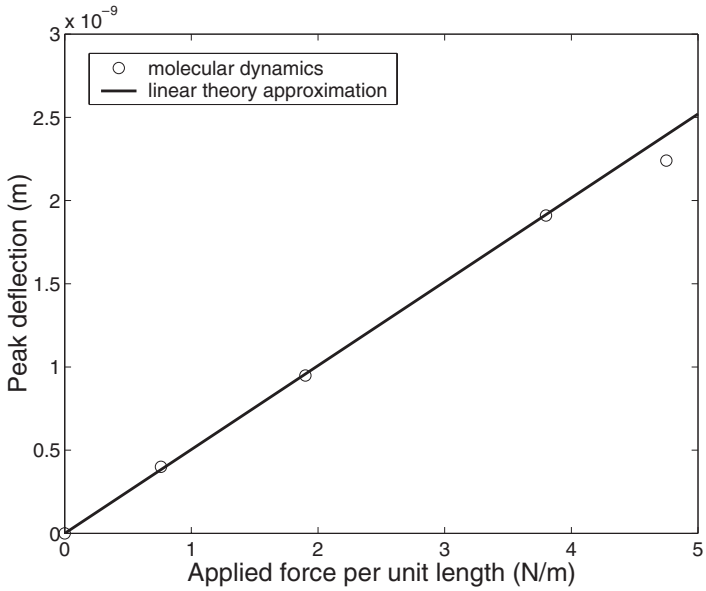

Figure 5. Peak deflection versus applied force for a fixed–fixed DWNT with a diameter of 1.96 nm and a length of 20 nm. The circles are MD data and the solid line is a linear approximation to the data.

4.2. Limitations of the beam theory

For very large loads, the stress concentration at the edges of the nanotubes may cause the tube to buckle and form kinks. In such cases, the deflection deviates from the beam theory locally. The buckling happens at a certain strain depending on the device geometry, the NT symmetry and the load. If buckling is to be simulated, one can try advanced continuum theories, such as a shell theory [27].

We have performed MD simulation on a DWNT with a diameter of 1.96 nm and a length of 10 nm. In this case we observed that the deflection predicted by the beam theory is less than the deflection predicted by the MD simulation. A DWNT of the same diameter and twice as long, however, produces a good agreement. One possible reason for the disagreement for the 10 nm long nanotube is that the aspect ratio is too small to apply the continuum beam approximation. Our results show that a good agreement between the beam theory and the MD simulations is observed if the length/diameter ratio is larger than 10.

From figure 5, it can be noticed that the deflection for larger loads can no longer be modelled by linear theory. In such cases, one can parametrize nonlinear continuum theories to model nanotube deflections.

4.3. Validation of continuum van der Waals theory

The continuum van der Waals model for an SWNT over a graphene ground plane (ground electrode) given in equation (3) is compared with the direct pairwise summation of the Lennard-Jones potential given in equation (1). We consider a (16, 0) tube. As shown in figure 6, the discrete theory agrees fairly well with the continuum theory—the deviation is below 1% at a shortest distance of 5 Å. Because the repulsion term is not taken into account, one cannot go below 5 Å. The multiple-shell continuum theory given in equation (4) has the same accuracy as the single-shell model. From this, we can conclude that continuum theory given in equations (3), (4) is a good approximation to model NEM switches when the sticking process is not considered.

5. Analytical expression for pull-in voltage

An analytical expression for the pull-in voltage of MEM switches has been published in [28]. In this paper, we extend the analysis presented in [28] to derive an analytical expression for the pull-in voltage of NEM switches. To derive the analytical pull-in voltage, the geometry shown in figure 1 is simplified to a one-dimensional lumped model as shown in figure 7. In the lumped model, the NEM switch is approximated by a rigid beam suspended over a ground plane. Thus, the only degree of freedom of the system is the uniform gap, r, between the plate and the ground plane. This gap is defined to be the gap between the tip of the cantilever structure and the ground plane for the cantilever switch and the gap between the centre of the fixed–fixed structure and the ground plane for a fixed–fixed switch.

As a further simplification, the beam is treated as a filled narrow rectangle. The thickness, t, of the rectangle (or the plate) is equal to the diameter of the tube and the width, w, is defined by matching the moment of inertia with the circular geometry. The van der Waals energy is estimated by using equation (2). The two volumes of integration are the semi-infinite ground electrode and a rectangular beam. With these simplifications, the van der Waals energy is given by

$$E_{\mathrm{vdW}} = -\frac{\pi \mathcal{C}_6 \rho^2 w L}{12}\left[\frac{1}{(r+t)^2} - \frac{1}{r^2}\right] \qquad (11)$$

where r is the distance between the plate and the ground plane, and ρ is the volume density of graphite, which is taken to be $\rho = 1.14 \times 10^{29}\ \mathrm{m}^{-3}$. The van der Waals force is then given

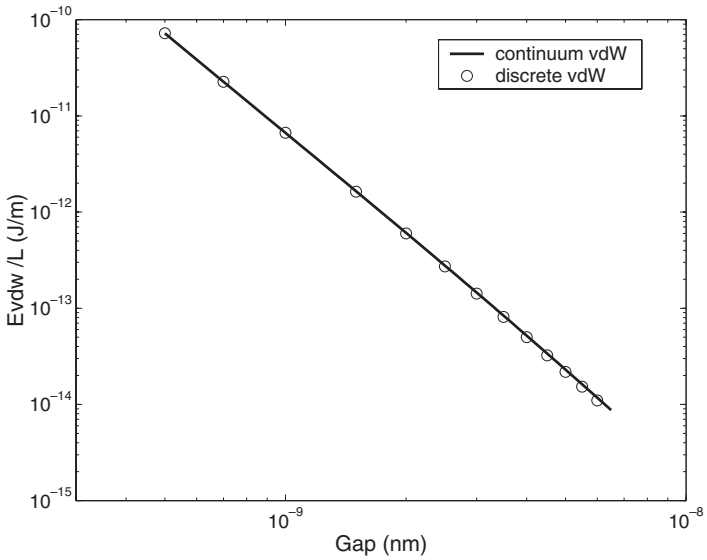

Figure 6. Comparison of the continuum van der Waals energy given by equation (3) with the discrete pairwise summation given by equation (1).

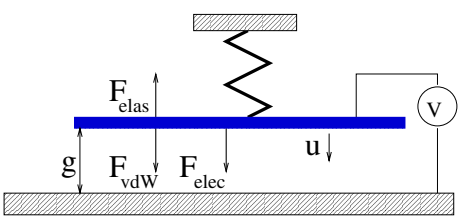

Figure 7. One-dimensional lumped model for pull-in voltage estimation. The deflection of the plate is given by u, and $r = g - u$.

by

$$F_{\mathrm{vdW}} = -\frac{\pi \mathcal{C}_6 \rho^2 w L}{6}\left[\frac{1}{r^3} - \frac{1}{(r+t)^3}\right]. \tag{12}$$

For the parallel plate configuration shown in figure 7, the electrostatic energy (accounting for fringing fields) is given by

$$F_{\mathrm{elec}} = \frac{\epsilon_0 w L V^2}{2r^2}\left(1 + \frac{2r}{\pi w}\right) \tag{13}$$

where the first term is the capacitance of a parallel plate and the second term is the fringing field correction [29].

The elastostatic restoring force is modelled by using an effective spring stiffness, i.e. the restoring force, F_{elas}, varies linearly with the deflection. The spring constant, k, is defined in the continuum model as $k = F/r_{\max}$, where F is the uniform force applied on the beam and $r_{\max}$ is the maximum deflection of the beam. Thus, the spring constant depends on the cross-sectional shape as well as on the boundary conditions. Considering a one-dimensional beam model, the spring constant is $k = 8EI/L^3$ for a cantilever beam and $k = 384EI/L^3$ for a fixed–fixed beam (L is the length of the beam, E is the Young's modulus and I is the moment of inertia).

For MEMS analysis [28], it was assumed that pull-in occurs when the structure deflects to 2/3 of the initial gap g. Even though the van der Waals forces can be expected to correct the MEMS result, we assume that this correction is negligible here. The pull-in voltage can be computed by solving $F_{\mathrm{elas}} + F_{\mathrm{elec}} + F_{\mathrm{vdW}} = 0$ at the equilibrium position. With a one-dimensional lumped model, the expression for pull-in voltage is given by

$$V_{\mathrm{PI}} = \sqrt{\left[k(g - r_{\mathrm{eq}}) - \frac{\pi \mathcal{C}_6 \rho^2 w L}{6}\left(\frac{1}{r_{\mathrm{eq}}^3} - \frac{1}{(r_{\mathrm{eq}}+t)^3}\right)\right] \times \frac{2r_{\mathrm{eq}}^2}{\left(1 + \frac{2r_{\mathrm{eq}}}{\pi w}\right) w L \epsilon_0}} \tag{14}$$

where V_{PI} is the pull-in voltage and $r_{\mathrm{eq}} \sim \frac{2}{3}g$ is the gap at which the pull-in occurs. In equation (14), the first term in the square brackets is the contribution of the elastostatic force and the second term is the contribution of the van der Waals force to the pull-in voltage. The forces are overestimated because the electrostatic and van der Waals forces are computed using the uniform gap. Thus, the overall result, given by the one-dimensional lumped model, underestimates the pull-in voltage of the device to some extent (this is discussed in more detail in section 6).

Scaling each characteristic length of the system by a factor of l in equation (14), the elastostatic contribution scales as l and the van der Waals contribution scales as $1/\sqrt{l}$. This scaling analysis of the pull-in voltage demonstrates that the van der Waals contribution becomes insignificant as the size of the system increases. Thus, the pull-in voltage itself scales as the length of the device.

If we neglect the van der Waals contribution in the above analysis, the pull-in voltage is given by

$$V_{\mathrm{PI}} = \sqrt{k(g - r_{\mathrm{eq}}) \times \frac{2r_{\mathrm{eq}}^2}{\left(1 + \frac{2r_{\mathrm{eq}}}{\pi w}\right) w L \epsilon_0}}. \tag{15}$$

In addition, if the fringing fields are neglected, the expression for the pull-in voltage is given by (by substituting $r_{\mathrm{eq}} \simeq \frac{2}{3}g$)

$$V_{\mathrm{PI}} = \sqrt{\frac{8kg^3}{27\epsilon_0 w L}}. \tag{16}$$

Equation (16) is identical to the pull-in voltage expression derived in [28] for MEMS.

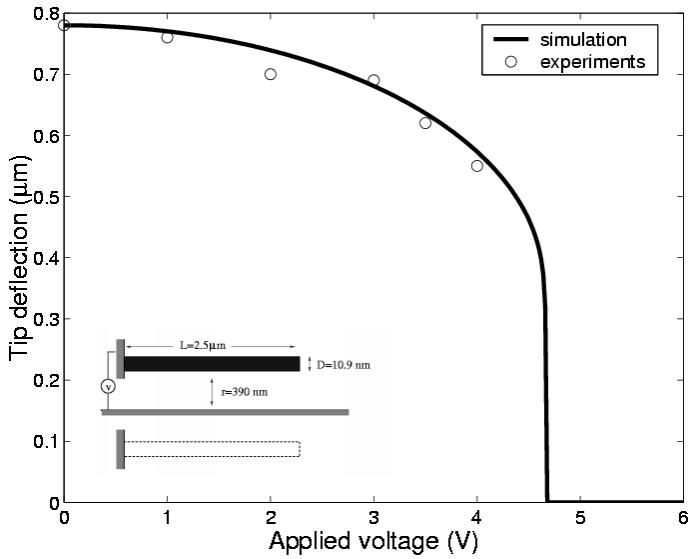

Figure 8. Tip deflection as a function of the applied voltage for a nanotweezers problem. The experimental data are from [6]. Inset: the model geometry.

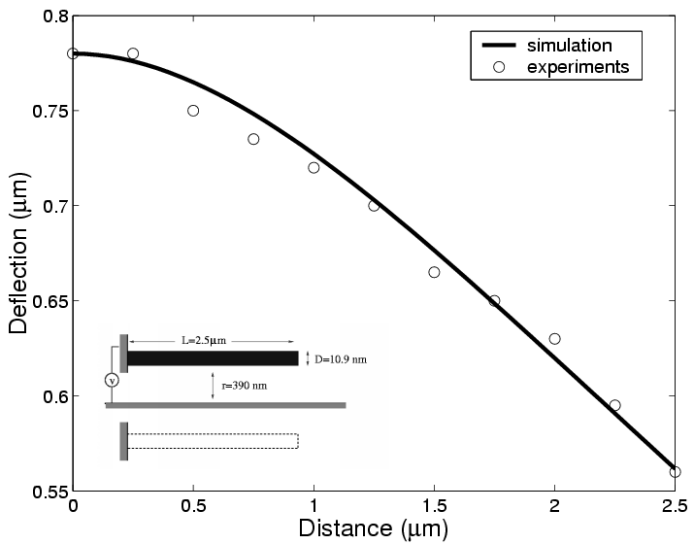

Figure 9. Deflection of the nanotweezers for an applied potential of 4 V. The experimental data are from [6]. Inset: the model geometry.

6. Results and discussion

All the simulation results presented in this section are obtained by solving equation (10). The electrostatic forces are computed with equation (7) and the van der Waals forces are computed with equation (5) (considering 30 sheets of graphene). When the van der Waals forces are neglected, q_{vdW} is set to zero in equation (10). For all the examples, except for the nanotweezers problem discussed in section 6.1, $E = 1.2$ TPa and $\epsilon_0 = 8.854 \times 10^{-12}$ C^2 N^{-1} m^{-2}.

6.1. Nanotweezers problem

The first example we investigate is the nanotweezers problem. Experimental data on the nanotweezers problem have been reported recently in [6]. The length of the tweezers is 2.5 μm and the gap between the two tweezers is 780 nm. The diameter of the nanotube was not experimentally measured. Akita *et al* [6] theoretically estimated a diameter of 13.3 nm. The Young's modulus has been taken to be 1 TPa in [6].

The inset in figure 8 shows the geometry used in our calculations. Using the continuum model presented in this paper, we were able to obtain a good match with experimental data with a diameter of 10.9 nm. Because of the large gap between the two tweezers, the van der Waals forces are negligible. The tip deflection as a function of the applied voltage is shown in figure 8. The experimental data from [6] are also shown in figure 8. The computed pull-in voltage is 4.65 V. Figure 9 shows a comparison between the experimentally measured and simulated deflection when a potential of 4 V

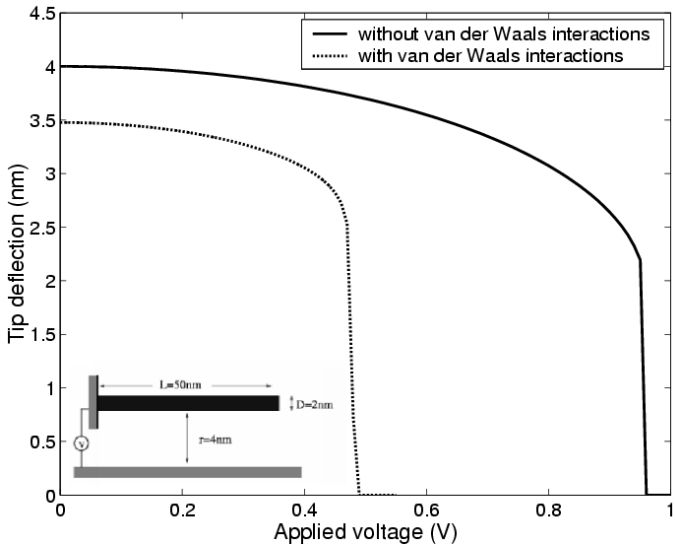

Figure 10. Tip deflection as a function of the applied voltage for a cantilever switch. Inset: the geometry of the cantilever switch.

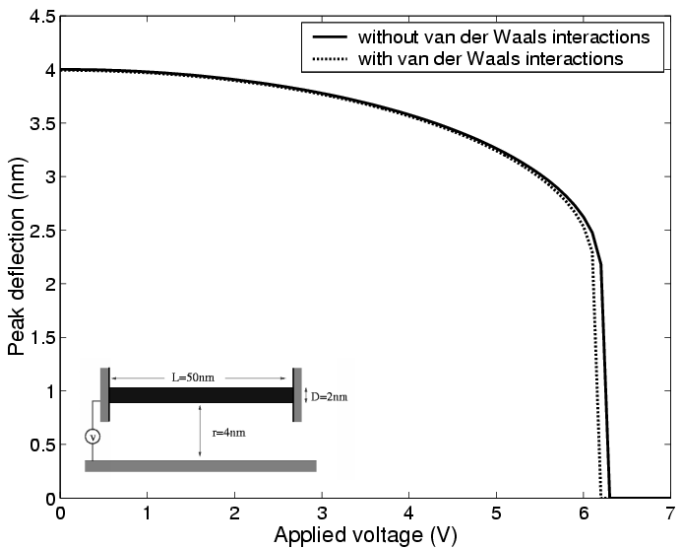

Figure 11. Peak deflection (which is at the centre of the nanotube) as a function of the applied voltage for a fixed–fixed switch. Inset: the geometry of the fixed–fixed switch.

is applied. We believe that our theoretical result, which uses a more accurate model compared with [6], is more precise in the description of this experiment.

The above example demonstrates that our continuum model does a reasonably good job in predicting the electromechanical behaviour of nanotweezers.

6.2. Cantilever switch

The next example we consider is a DWNT cantilever switch. The geometry of the switch is shown as an inset in figure 10. The DWNT is 50 nm long, and has a diameter of 2 nm ($R_{\text{ext}} = 10$ Å and $R_{\text{int}} = 6.65$ Å) and is positioned 4 nm above the ground plane. The tip deflection as a function of the applied voltage is shown in figure 10. When the van der Waals forces are neglected, the pull-in voltage is 0.97 V. When the van der Waals forces are taken into account, the pull-in voltage reduces to 0.48 V.

We have repeated the same simulation with a larger gap (10 nm) but with the same length and diameter. The pull-in voltage is computed to be 3.0 and 3.1 V, respectively, with and without the van der Waals forces. In this case, we have noticed that the effect of the van der Waals interaction is negligible. From this example, we can conclude that for smaller gaps the van der Waals forces play an important role in determining the deflections as well as the pull-in voltage of cantilever switches.

6.3. Fixed–fixed switch

We have also simulated a DWNT fixed–fixed switch with a length of 50 nm, diameter of 2 nm and a gap of 4 nm. The geometry is shown as the inset in figure 11. Compared with a cantilever geometry, fixing both ends of the tube makes the tube stiffer and results in smaller deflections. The results for

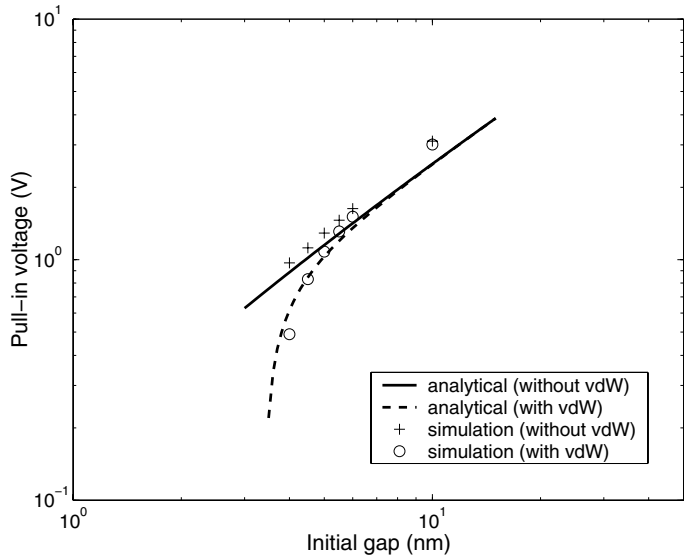

Figure 12. Variation of the pull-in voltage with gap for cantilever switches with a length of 50 nm and a diameter of 2 nm.

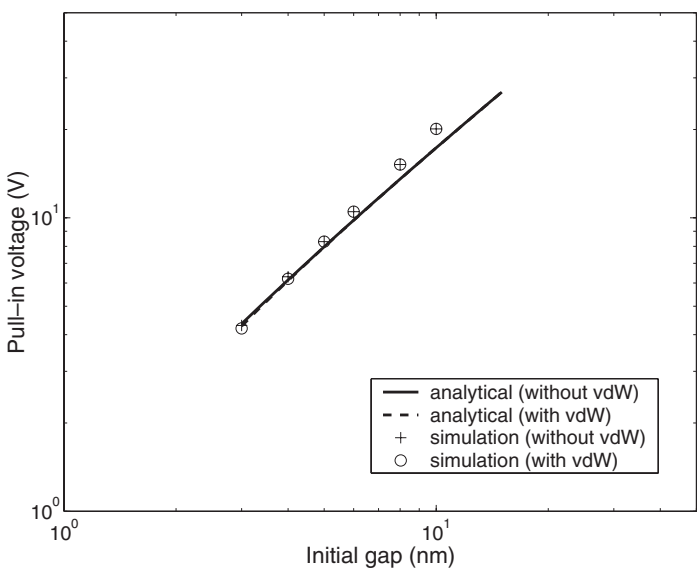

Figure 13. Variation of the pull-in voltage with gap for fixed–fixed switches with a length of 50 nm and a diameter of 2 nm.

the fixed–fixed switch are summarized in figure 11. First, we observe that the pull-in voltage required to collapse the fixed–fixed tube is 6.3 V, which is much higher compared with the cantilever switch. In addition, we observe that the van der Waals interactions are not significant. The pull-in voltage computed by including the van der Waals forces is 6.2 V. From this example, we can conclude that even at a small gap, the van der Waals interactions are not significant for fixed–fixed tubes.

6.4. Comparison of analytical pull-in voltage with simulations

We have considered cantilever and fixed–fixed switches with varying lengths, diameters and gaps and compared the pull-in voltages obtained with the analytical expressions given in section 5 and the continuum model simulations. In figures 12–17, the analytical pull-in voltage with and without the van der Waals forces is computed by using equations (14) and (15), respectively.

Considering a length of 50 nm and a diameter of 2 nm, the variation of the pull-in voltage with gap for cantilever and fixed–fixed switches is shown in figures 12 and 13, respectively. As the gap decreases the pull-in voltage decreases. If the van der Waals forces are neglected, the slope of the pull-in voltage curve is fairly constant (on a log–log scale). However, when van der Waals forces are taken into account, the slope changes rapidly at small gaps, producing significantly lower pull-in voltages. A noticeable deviation of the analytical formula from the simulation result at larger gaps may be due to the assumptions used in the derivation of the analytical formula—specifically, a planar capacitor is used

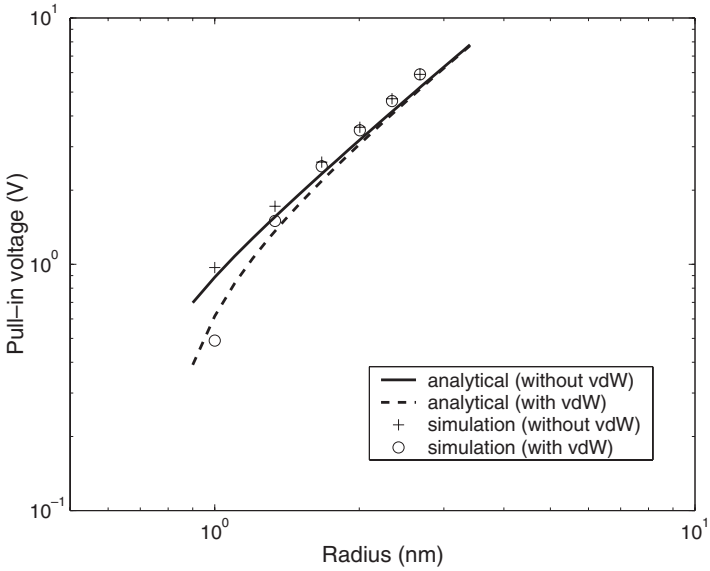

Figure 14. Variation of the pull-in voltage with tube diameter for cantilever switches with a length of 50 nm and a gap of 4 nm.

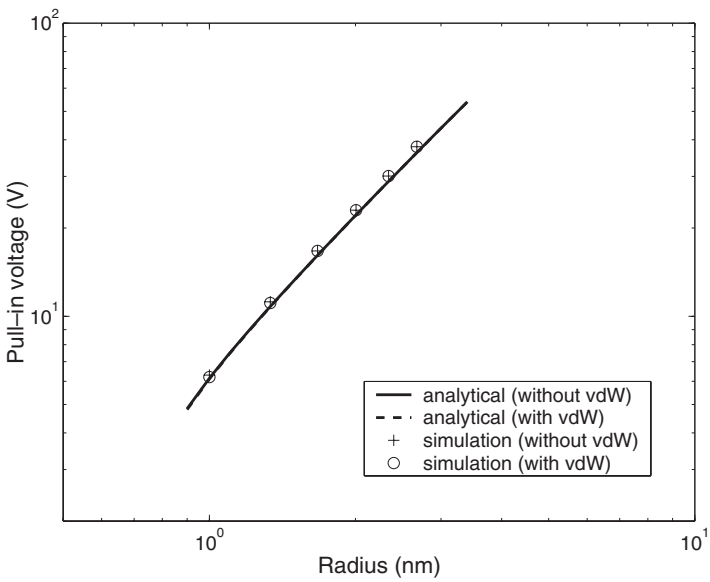

Figure 15. Variation of the pull-in voltage with tube diameter for fixed–fixed switches with a length of 50 nm and a gap of 4 nm.

instead of the cylindrical capacitor. Defining a critical gap to be the distance at which the tube pulls in (because of the van der Waals interactions) without any applied voltage, we observe that the analytical expression for the pull-in voltage captures the critical gap. For a cantilever switch with a length of 50 nm and a diameter of 2 nm, we find that the critical gap is 3.5 nm. The critical gap is an important parameter for the design of NEM switches as it defines the smallest operable gap. For identical geometries, fixed–fixed switches have smaller critical gaps compared with cantilever switches as fixed–fixed switches are a lot stiffer.

Figures 14 and 15 show the variation of the pull-in voltage as a function of the tube diameter for cantilever and fixed–fixed switches, respectively, when the length of the tube is 50 nm and the initial gap is 4 nm. As the diameter increases, the pull-in voltage increases. For fixed–fixed switches we again observe an excellent match between analytical and simulated pull-in voltages. In addition, the van der Waals interactions do not play a significant role. For cantilever switches, we get a reasonably good match between analytical and simulated pull-in voltages. As the tube diameter gets smaller, the van der Waals interactions start playing an important role in determining the pull-in voltages.

Figures 16 and 17 show the variation of the pull-in voltage as a function of the tube length for cantilever and fixed–fixed switches, respectively, when the diameter of the tube is 2 nm and the initial gap is 4 nm. In this study, R_{int} is fixed at 6.65 Å and the number of outer shells grows along with the tube radius. Each additional outer shell increases the radius by 3.35 Å. As the length increases, the pull-

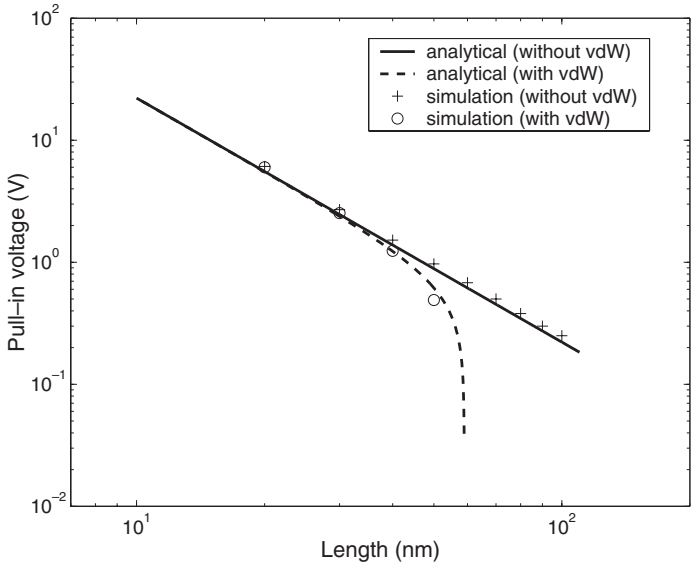

Figure 16. Variation of the pull-in voltage with length of the tube for cantilever switches with a diameter of 2 nm and an initial gap of 4 nm.

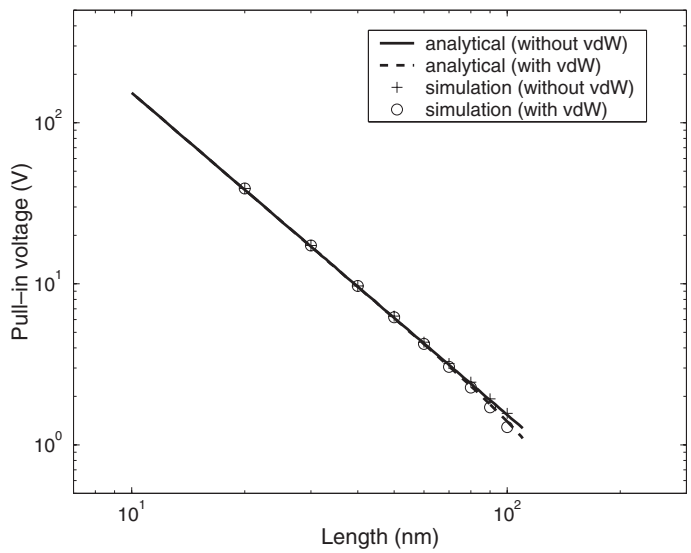

Figure 17. Variation of the pull-in voltage with length of the tube for fixed–fixed switches with a diameter of 2 nm and an initial gap of 4 nm.

in voltage decreases. For fixed–fixed switches we observe an excellent match between analytical and simulated pull-in voltages. In addition, van der Waals interactions do not play a significant role. For cantilever switches, we get a good match between analytical and simulated pull-in voltages. As the tube length increases, the van der Waals interactions again play an important role in determining the pull-in voltage.

From the above results, we conclude that the analytical expression for pull-in voltage provides a quick and accurate estimation of the pull-in voltage for cantilever and fixed–fixed switches.

7. Conclusion

A continuum model for the simulation of carbon-nanotube-based NEM switches is proposed in this paper. In particular, a parametrized beam model is shown to provide good results for mechanical behaviour of NEM switches. The Young's modulus required in the beam equation is extracted from MD simulations. A continuum model is also proposed to compute van der Waals interactions. The continuum model for the van der Waals interactions provides a good accuracy when compared with the discrete Lennard-Jones model. Numerical results with the continuum model for a nanotweezer problem compare well with the experimental data. Pull-in voltages for several cantilever and fixed–fixed DWNT switches are computed by using the continuum model. Results indicate that the van der Waals force can play a significant role in determining the pull-in voltage of cantilever switches for small gaps. A fixed–fixed switch is less sensitive to the van der Waals force and can operate with much smaller gaps. An analytical expression, based on a lumped model, is derived to estimate the pull-in voltage of cantilever and fixed–fixed switches.

Acknowledgments

This work is supported by a National Science Foundation SGER grant CCR 0107623 and by a Critical Research Initiatives (CRI) Program at the University of Illinois at Urbana-Champaign. This support is gratefully acknowledged. SVR acknowledges the Arnold and Mabel Beckman foundation for the Beckman fellowship.

References

[1] Kovacs G T A 1998 *Micromachined Tranducers Sourcebook* (New York: McGraw-Hill)
[2] Rueckes T, Kim K, Joselevich E, Tseng G Y, Cheung C-L and Lieber C M 2000 Carbon nanotube-based nonvolatile random access memory for molecular computing *Science* **289** 94–7
[3] Kim P and Lieber C M 1999 Nanotube nanotweezers *Science* **286** 2148–50
[4] Collins P G, Bradley K B, Ishigami M and Zettl A 2000 Extreme oxygen sensitivity of electronic properties of carbon nanotubes *Science* **287** 1801–4
[5] Adu C K W, Sumanasekera G U, Pradhan B K, Romero H E and Eklund P C 2001 Carbon nanotubes: a thermoelectric nano-nose *Chem. Phys. Lett.* **337** 31–5
[6] Akita S *et al* 2001 Nanotweezers consisting of carbon nanotubes operating in an atomic force microscope *Appl. Phys. Lett.* **79** 1691–3
[7] Baughman R H *et al* 1999 Carbon nanotube actuators *Science* **284** 1340–4
[8] Srivastava D, Menon M and Cho K 2001 Computational nanotechnology with carbon nanotubes and fullerenes *Comput. Sci. Eng.* **3** 42–55
[9] Han J, Globus A, Jaffe R and Deardorff G 1997 Molecular dynamics simulations of carbon nanotube-based gears *Nanotechnology* **8** 95–102
[10] Li G and Aluru N R 2001 Linear, nonlinear and mixed-regime analysis of electrostatic MEMS *Sensors Actuators* A **91** 278–91
[11] Aluru N R and White J 1997 An efficient numerical technique for electromechanical simulation of complicated microelectromechanical structures *Sensors Actuators* A **58** 1–11
[12] Aluru N R and White J 1999 A multilevel Newton method for mixed-energy domain simulation of MEMS *J. MEMS* **8** 299–308
[13] Lennard-Jones J E 1930 Perturbation problems in quantum mechanics *Proc. R. Soc.* A **129** 598–615
[14] Girifalco L A, Hodak M and Lee R S 2000 Carbon nanotubes, buckyballs, ropes, and a universal graphitic potential *Phys. Rev.* B **62** 13 104–10
[15] Girifalco L A 1992 Molecular properties of C_{60} in the gas and solid phases *J. Phys. Chem.* **96** 858–61
[16] Jackson J D 1998 *Classical Electrodynamics* 3rd edn (New York: Wiley)
[17] Hayt W H 1981 *Engineering Electromagnetics* 4th edn (New York: McGraw-Hill)
[18] Salvetat J P *et al* 1999 Elastic modulus of ordered and disordered multiwalled carbon nanotubes *Advanced Mater.* **11** 161–5
[19] Wong E W, Sheehan P E and Lieber C M 1997 Nanobeam mechanics elasticity, strength, and toughness of nanorods and nanotubes *Science* **277** 1971–5
[20] Allen M P and Tildesley D J 1987 *Computer Simulation of Liquids* (Oxford: Oxford University Press)
[21] Brenner D W 1990 Empirical potential for hydrocarbons for use in simulating the chemical vapor deposition of diamond films *Phys. Rev.* B **42** 9458–71
[22] Van Lier G, Van Alsenoy C, Van Doren V and Geerlings P 2000 Ab initio study of the elastic properties of single-walled carbon nanotubes and graphene *Chem. Phys. Lett.* **326** 181–5
[23] Treacy M M J, Ebbesen T W and Gibson J M 1996 Exceptionally high Young's modulus observed for individual carbon nanotubes *Nature* **381** 678–80
[24] Hernández E, Goze C, Bernier P and Rubio A 1998 Elastic properties of C and $B_xC_yN_z$ composite nanotubes *Phys. Rev. Lett.* **80** 4502–5
[25] Lu J P 1997 Elastic properties of carbon nanotubes and nanoropes *Phys. Rev. Lett.* **79** 1297–300
[26] Krishnan A, Dujardin E, Ebbesen T W, Yianilos P N and Treacy M M J 1998 Young's modulus of single-walled nanotubes *Phys. Rev.* B **58** 14 013–19
[27] Yakobson B I, Brabec C J and Berholc J 1996 Nanomechanics of carbon tubes: instabilities beyond linear response *Phys. Rev. Lett.* **76** 2511–14
[28] Osterberg P M 1995 Electrostatically actuated micromechanical test structures for material property measurement *PhD Dissertation* MIT, Cambridge, MA
[29] Osterberg P M and Senturia S D 1997 M-test: a test chip for MEMS material property measurement using electrostatically actuated test structures *J. MEMS* **6** 107–18